Peering towards Cosmic Dawn
Proceedings IAU Symposium No. 333, 2018
V. Jelić & T. van der Hulst, eds.

doi:10.1017/S174392131701122X

Wide-field LOFAR-LBA power-spectra analyses: Impact of calibration, polarization leakage and ionosphere

Bharat K. Gehlot[1]* and Léon V. E. Koopmans[2]

[1]Kapteyn Astronomical Institute, University of Groningen, PO Box 800, 9700AV Groningen, the Netherlands
*email: gehlot@astro.rug.nl

Abstract. Contamination due to foregrounds, calibration errors and ionospheric effects pose major challenges in detection of the cosmic 21 cm signal in various Epoch of Reionization (EoR) experiments. We present the results of a study of a field centered on 3C196 using LOFAR Low Band observations, where we quantify various wide field and calibration effects such as gain errors, polarized foregrounds, and ionospheric effects. We observe a 'pitchfork' structure in the power spectrum of the polarized intensity in delay-baseline space, which leaks into the modes beyond the instrumental horizon. We show that this structure arises due to strong instrumental polarization leakage (30%) towards Cas A which is far away from primary field of view. We measure a small ionospheric diffractive scale towards CasA resembling pure Kolmogorov turbulence. Our work provides insights in understanding the nature of aforementioned effects and mitigating them in future Cosmic Dawn observations.

Keywords. cosmology: observations, techniques: interferometric, polarization, techniques: polarimetric, atmospheric effects, methods: statistical

1. Introduction

Observations of 21-cm hyperfine transition of neutral Hydrogen (HI) at high redshifts promises to be an excellent probe of the HI distribution in the Inter-Galactic Medium (IGM) during the Cosmic Dawn (CD) and Epoch of Reionization (EoR) (Madau *et al.* (1997), Shaver *et al.* (1999), Furlanetto *et al.* (2006), Pritchard & Loeb (2012), Zaroubi (2013)). Several ongoing and upcoming experiments such as the LOw Frequency ARray (LOFAR; van Haarlem *et al.* (2013)), the Giant Meterwave Radio Telescope (GMRT; Paciga *et al.* (2011)), the Murchinson Widefield Array (MWA; Tingay *et al.*, (2013), Bowman *et al.* (2013)), the Precision Array for Probing the Epoch of Reionization (PAPER; Parsons *et al.* (2010)), the 21 Centimeter Array (21CMA; Zheng *et al.* (2016)), the Hydrogen Epoch of Reionization Array (HERA; DeBoer (2015)) and the Square Kilometer Array (SKA; Mellema *et al.* (2013), Koopmans *et al.* (2015)) aim to detect the redshifted 21-cm emission from the EoR. Although the above instruments focus largely on detecting the EoR, LOFAR-LBA, the upcoming NENUFAR (New Extension in Nançay Upgrading loFAR; Zarka *et al.* (2012)) and SKA-low also observe at frequencies (50-80 MHz) range which corresponds to a part of the redshift range of the CD ($30 \gtrsim z \gtrsim 15$).

The expected 21-cm signal from $z = 30$ to 15 is extremely faint and is buried deep below galactic and extra-galactic foreground emission which dominate the sky at these low frequencies. Contamination due to the (polarized) foregrounds, ionospheric propagation effects and systematic biases (e.g. station-beam errors) pose considerable challenges in the detection of this signal. It is crucial to remove these bright foregrounds and mitigate other effects accurately in order to obtain a reliable characterization of the 21-cm signal

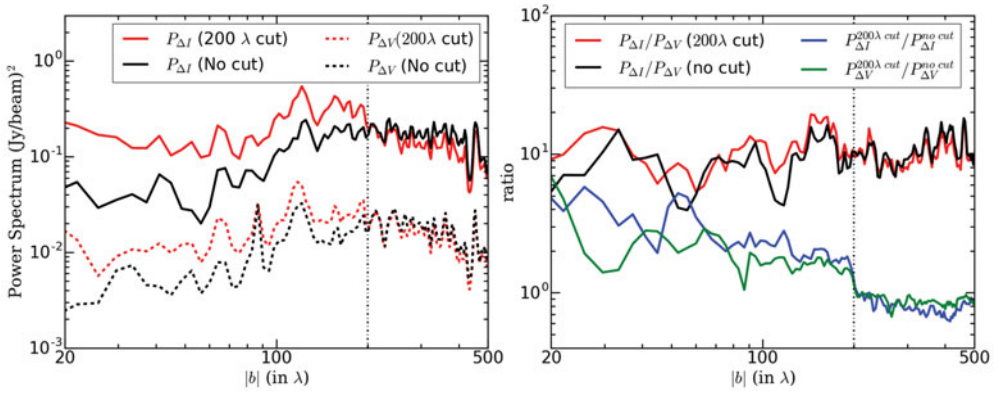

Figure 1. The left panel shows the differential Stokes I and V power spectra for the two calibration schemes. Right panel shows the ratios of different combinations of $P_{\Delta I}$ and $P_{\Delta V}$.

(e.g. power spectrum). This requires a detailed understanding of the nature of these effects and the errors associated with these effects. We study challenges for observing the CD with LOFAR, and it's implications on the future SKA-Low which will largely have a similar layout. Using the LOFAR Low Band Antenna (LBA) observations of a field centered on 3C196 (3C196 field hereafter), we study some of the aforementioned effects at lower frequency range (56-70 MHz) covering part of the CD, where both the foregrounds and ionospheric effects are known to be even stronger.

We use use 8 hours of synthesis observation of the 3C196 field using LOFAR-Low Band Antenna (LBA) system for our analysis (refer to van Haarlem *et al.* (2013) for more information about LOFAR capabilities). 3C196 field is one of the two primary observation windows of the LOFAR EoR Key Science Project (Patil *et al.* (2017)). The field was observed with 37 LOFAR-LBA stations in the Netherlands (70 m to 80 km baseline) operating in the frequency range of 30-78 MHz. Observed data was processed using the standard LOFAR software pipeline. The data processing steps include flagging and averaging, calibration (Direction Independent (DI) and Direction Dependent (DD)), imaging and source modeling. See Gehlot *et al.* (2017) for more details about the data processing steps.

2. Results and Discussions

We use different statistical techniques such as differential Stokes power spectrum, delay spectrum and cross-coherence to study and quantify various signal contamination effects e.g. systematic biases (excess variance in Stokes I images vs. Stokes V images), polarization leakage and ionospheric effects. These techniques are summarized below.
Diffrential power spectrum: Azimuthally averaged power spectrum of the difference between the Stokes images of adjacent subbands (differential Stokes images, hereafter) may be used to quantify the effects which are non-smooth in frequency (on subband level) such as instrumental and calibration effects. Figure 1 shows $P_{\Delta I}$ and $P_{\Delta V}$ for the both calibration schemes. We observe a factor ~ 10 larger power (i.e. $\sim 3\times$ larger rms) in differential Stokes I than Stokes V for both calibration strategies (figure 1 right panel). This ratio is constant as a function of baseline length and does not change between the two calibration strategies we employed. Figure 1 right panel shows the ratio $P_{\Delta I}(200\lambda\text{ cut})/P_{\Delta I}(\text{no cut})$ and $P_{\Delta V}(200\lambda\text{ cut})/P_{\Delta V}(\text{no cut})$. We observe that both ratios have a discontinuity at the exact location of the calibration cut. The excess noise suddenly is $\gtrsim 2$ times higher

https://doi.org/10.1017/S174392131701122X Published online by Cambridge University Press

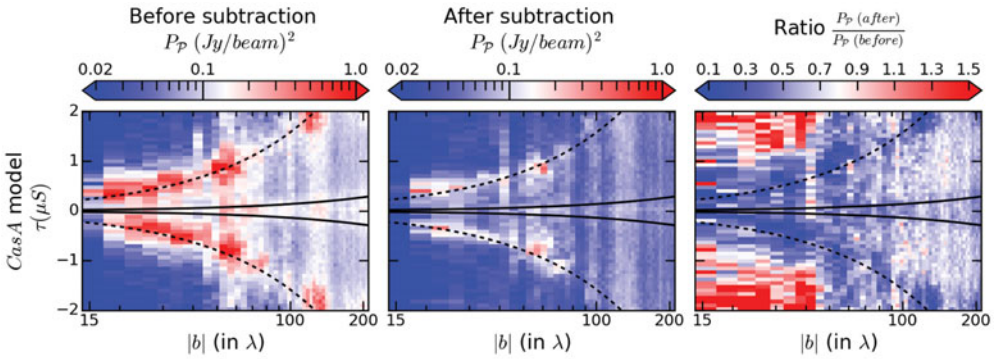

Figure 2. Polarized intensity $\mathcal{P}$ delay power spectra before (left column) and after (center column) Cas A model subtraction and their ratio (right column). This figure is adapted from Gehlot *et al.* (2017)

on baselines $< 200\lambda$ than baselines $> 200\lambda$. We expect this effect to be purely because of the calibration cut. We expect that this discontinuity is the result of random errors introduced in the Jones matrices during the calibration process, which are subsequently applied to the sky model and transferred to the image residuals during model subtraction. The cause of these random gain errors on the longer baselines could be due to sky model incompleteness or the ionosphere (Patil *et al.*, (2016), Barry *et al.* (2016), Ewall-Wice *et al.* (2017)).

Delay Spectrum: The Delay spectrum is a powerful tool to study foregrounds and various contamination effects which can leak foregrounds into the EoR-window. We determine the delay power spectrum from the Stokes I, Q, U, V images produced before and after DD-calibration step using 200λ cut strategy where only CasA is subtracted. We observe a 'pitchfork' structure in the delay spectrum of total polarized intensity $\mathcal{P}$ ($P_{\mathcal{P}}$) (shown in left panel of figure 2). Most of this polarized emission is localized on smaller baselines ($\leqslant 80\lambda$) and around the delays corresponding to instrumental horizon suggesting that the emission originates from far outside the primary beam and is diffuse in nature. This can either be caused by genuine diffuse polarized emission or instrumental polarization leakage from Stokes I to Q and U. We compare $P_{\mathcal{P}}$ before and after subtracting CasA (using DD calibration) which lies outside the primary beam. Figure 2 shows the comparison between $P_{\mathcal{P}}$ before and after subtracting CasA. It is clear that subtraction of CasA has a significant impact on the polarized intensity $\mathcal{P}$ around the horizon delay line and also on the modes within the horizon lines as well as far beyond the horizon. The residuals after subtracting CasA still correlate quite strongly with the power before CasA subtraction, suggesting imperfect subtraction in DD calibration or that the structure of CasA is difficult to model. Ionospheric turbulence can also cause CasA to scintillate significantly and visibilities to decorrelate within the DD calibration solution interval. This 'scintillation noise' (see e.g. Vedantham & Koopmans (2015), Vedantham & Koopmans (2016)) therefore might lead to imperfect calibration causing residual flux.

Ionospheric Scintillation: We observed residual flux in $\mathcal{P}$ delay spectrum even after subtraction of CasA. Given the low-frequency and large angle away from zenith (i.e. large vTEC), we expect CasA to be strongly affected by the ionosphere. The power spectrum of an unresolved source as a function of baselines is constant in absence of ionospheric effects. However if the source is affected by the ionosphere, it will take the form of power spectrum of a source affected by Kolmogorov turbulence (Vedantham & Koopmans (2015), Vedantham & Koopmans (2016)) in ionosphere. We find that zero delay

https://doi.org/10.1017/S174392131701122X Published online by Cambridge University Press

power spectrum of Cas A fits very well with the Kolmogorov turbulence power spectrum. We find a diffractive scale $r_{\rm diff}$ (free parameter in the fit) towards CasA of order $\sim 80\lambda$ or equivalently ~ 400 m at 60 MHz for both P_I and $P_{\mathcal{P}}$. We also notice that the residuals in $P_{\mathcal{P}}$ after Cas A subtraction are incoherent over 5 min intervals as expected for ionospheric scintillation noise. Readers may refer to Gehlot *et al.* (2017) for detailed analysis of ionospheric scintillation.

3. Summary

The contamination effects which we have discussed are in part identified in LOFAR-HBA data at frequencies around 150 MHz, but they appear much stronger in LOFAR-LBA data. This might be partly due to the small diffractive scale of the ionosphere, but also due to the calibration process and the incomplete sky model. These and other far-field effects (such as scintillation of CasA) need to be accounted for before the thermal noise (or Stokes V rms) level can be reached at frequencies relevant for 21-cm CD observations. In upcoming CD experiments such as SKA-low and NENUFAR which will observe in the frequency range of 30 to 80 MHz and will probe the same short baselines as studied here, these effects have to be mitigated to an accuracy of $\sim 0.01\%$ or be incoherent and below the thermal noise such that they average down in time in order to get a detection. This study will prove to be helpful in understanding the nature of these contamination effects as well as their behavior at low frequencies.

References

Barry, N., Hazelton, B., Sullivan, I., Morales, M. F., & Pober, J. C., 2016, *MNRAS*, 461, 3135
Bowman, J. D., *et al.*, 2013, *Publ. Astron. Soc. Australia*, 30, e031
DeBoer D. R., 2015, *in American Astronomical Society Meeting Abstracts*, p. 328.03
Ewall-Wice, A., Dillon, J. S., Liu, A., & Hewitt, J., 2017, *MNRAS*, 470, 1849
Furlanetto, S. R., Oh, S. P., & Briggs, F. H., 2006, *Phys. Rep.*, 433, 181
Gehlot, B. K., Koopmans, L., *et al.*, 2017, arXiv 1709.07727
Koopmans, L., *et al.*, 2015, *Advancing Astrophysics with the Square Kilometre Array (AASKA14)*, p. 1
Madau P., Meiksin A., & Rees M. J., 1997, *ApJ*, 475, 429
Mellema, G., *et al.*, 2013, *Experimental Astronomy*, 36, 235
Paciga, G., *et al.*, 2011, *MNRAS*, 413, 1174
Parsons, A. R., *et al.*, 2010, *AJ*, 139, 1468
Patil, A. H., *et al.*, 2016, *MNRAS*, 463, 4317
Patil, A. H., *et al.*, 2017, *ApJ*, 838, 65
Pritchard, J. R. & Loeb A., 2012, *Reports on Progress in Physics*, 75, 086901
Shaver, P. A., Windhorst, R. A., Madau P., & de Bruyn A. G., 1999, *A&A*, 345, 380
Tingay, S. J., *et al.*, 2013, *Publ. Astron. Soc. Australia*, 30, e007
Vedantham, H. K. & Koopmans L. V. E., 2015, *MNRAS*, 453, 925
Vedantham H. K., Koopmans L. V. E., 2016, *MNRAS*, 458, 3099
Zarka, P., Girard, J. N., Tagger, M., & Denis, L., 2012, in Boissier S., de Laverny P., Nardetto N., Samadi R., Valls-Gabaud D., Wozniak H., eds, *SF2A-2012: Proceedings of the Annual meeting of the French Society of Astronomy and Astrophysics.*, pp 687–694
Zaroubi, S., 2013, *in Wiklind T., Mobasher B., Bromm V., eds, Astrophysics and Space Science Library*, Vol. 396, The First Galaxies. p. 45 arXiv 1206.0267
Zheng, Q., Wu, X.-P., Johnston-Hollitt, M., Gu, J.-h., & Xu H., 2016, *ApJ*, 832, 190
van Haarlem, M. P., *et al.*, 2013, *A&A*, 556, A2

https://doi.org/10.1017/S174392131701122X Published online by Cambridge University Press